

Surface Dissolution and Formation of Scallops



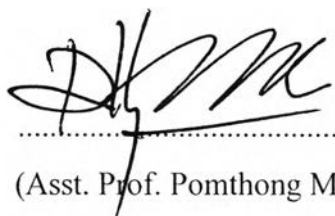
Mr.Pasit Warunphaisal

A Thesis Submitted in Partial Fulfilment of the Requirements
for the Degree of Master of Science
The Petroleum and Petrochemical College, Chulalongkorn University
in Academic Partnership with
The University of Michigan, The University of Oklahoma,
Case Western Reserve University and Institut Français du Pétrole
2009

522061

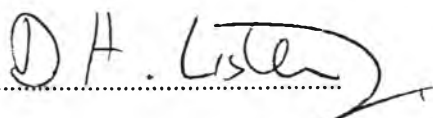
Thesis Title: Surface Dissolution and Formation and Scallops
By: Pasit Warunphaisal
Program: Petroleum Technology
Thesis Advisors: Assoc. Prof. Thirasak Rirksomboon
Prof. Derek H. Lister
Prof. Frank R. Steward


Accepted by the Petroleum and Petrochemical College, Chulalongkorn University, in partial fulfilment of the requirements for the Degree of Master of Science.



..... College Dean
(Asst. Prof. Pomthong Malakul)

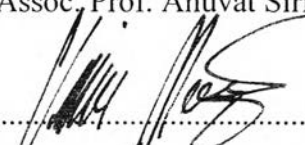
Thesis Committee:


.....
(Assoc. Prof. Thirasak Rirksomboon)


.....
(Prof. Derek H. Lister)


.....
(Prof. Frank R. Steward)


.....
(Assoc. Prof. Anuvat Sirivat)


.....
(Assoc. Prof. Vissanu Meeyoo)

ABSTRACT

5073006063: Petroleum Technology Program

Pasit Warunphaisal: Surface Dissolution and Formation of Scallops.

Thesis Advisors: Assoc. Prof. Thirasak Rirksomboon, Prof. Derek H.

Lister and Prof. Frank R. Steward

Keywords: Scallop Surface, Flow accelerated corrosion, Dissolution

Flow-assisted corrosion (FAC) is a significant problem with carbon steel components exposed to rapidly moving water or water-steam mixtures. Such components often develop distinctive patterns of surface damage producing a dimpled surface looking like orange peel, called “Scalloping”. This roughness plays an important role in the corrosion of pipes made of carbon steel and it seems that the formation of scallops are major factors in the thinning rate of the pipes. To characterize scallops, study the mechanisms of scallop formation and investigate how the formation of scallops and scallop phenomena affect the dissolution rate, experiments on the pressure drop and flow characteristics, of pipes made of plaster of Paris ($\text{CaSO}_4 \cdot 1/2\text{H}_2\text{O}$) were performed. Atomic Absorption Spectroscopy (AAS) was used to analyze the dissolution rate of the plaster. The surface was photographed with a digital camera to observe the initiation of scallops. Pressure transducer was used to measure pressure drop. The size decreases with increasing flow rate whereas the population of scallops increases with increasing flow rate. Scalloping is believed to initiate from defect at the surface and it was found that size and population of scallops increase with increasing initial defect size and initial defect concentration respectively. The average dissolution rate increases with increasing flow rate, particle size, particle concentration and temperature. The dissolution rate of plaster is controlled by mixed kinetics. The entrance section affected the mechanism of the gypsum dissolution. It is found that concentration of defects on the plaster surface has a greater effect on the dissolution rate than effect of defect size. Pressure drop increases with increasing flow rate and temperature but decreases with increasing initial defect size and concentration. This means that the diameter of the plaster pipe has a greater effect than the surface roughness.

บทคัดย่อ

ภายิต วรคุณไพศาล : ชื่อหัวข้อวิทยานิพนธ์ การสลายตัวของพื้นผิวและการก่อรูปสเกลลอปบนพื้นผิวท่อ (Surface Dissolution and Formation of Scallops) อ. ที่ปรึกษา : รศ. ดร. ธีรศักดิ์ ฤกษ์สมบูรณ์ ศ. ดร. ดีเรก เอช ลิสเตอร์ และ ศ. ดร. แฟรงค์ อาร์ สจ๊วต 129 หน้า

การกัดกร่อนแบบมีอัตราของของไหลเป็นตัวเร่ง (flow-accelerated corrosion) เป็นปัญหาสำคัญที่เกิดขึ้นกับท่อเหล็กคาร์บอนที่สัมผัสกับน้ำหรือส่วนผสมระหว่างน้ำและไอน้ำที่ไหลอย่างรวดเร็ว ท่อเหล็กคาร์บอนนี้มักจะเกิดความเสียหายบนพื้นผิวในแบบลักษณะพิเศษซึ่งจะสร้างพื้นผิวขรุขระลักษณะคล้ายเปลือกส้ม, เรียกว่า “สเกลลอป” ผิวขรุขระนี้มีบทบาทที่สำคัญในการกัดเซาะของท่อที่สร้างจากเหล็กคาร์บอนและดูเหมือนว่าการก่อรูปของสเกลลอปนี้จะเป็นตัวแปรหลักในอัตราการบางลงของท่อ การก่อเกิดสเกลลอปนี้เป็นปัญหาในการคำนวณอายุการใช้งานของท่อ และเครื่องมือ บ่อยครั้งที่สเกลลอปถูกนำมาใช้อย่างสอดคล้องกันในด้านความขรุขระที่ใช้น้ำในการขับเคลื่อน, การเพิ่มความดันลด และการถ่ายเทมวล ทั้งนี้เพื่อจะดูลักษณะพิเศษของสเกลลอป, ศึกษากลไกของการเกิดสเกลลอป, ศึกษาการเกิดสเกลลอปและปรากฏการณ์ของสเกลลอปว่าส่งผลอย่างไรต่ออัตราการสลายตัว, การศึกษาความดันลด และลักษณะของการไหล, การทดลองได้ถูกสร้างขึ้นจากท่อที่สร้างจากพลาสติกอะคริลิก (Plaster of Paris, $\text{CaSO}_4 \cdot 1/2\text{H}_2\text{O}$) เครื่องอะตอมมิคแอนะไลซิสอินดักทีฟ (AAS) ได้ถูกใช้เพื่อวิเคราะห์อัตราการสลายตัวของพลาสติก พื้นผิวถูกถ่ายภาพด้วยกล้องจุลทรรศน์เพื่อศึกษาการเกิดสเกลลอป เครื่องวัดความดันแบบแปรกระแสได้ถูกใช้เพื่อวัดความดันลด ผลปรากฏว่าลักษณะของสเกลลอปมีความสัมพันธ์กับอัตราการไหล ขนาดของสเกลลอปลดลงตามการเพิ่มขึ้นของอัตราการไหล ในขณะที่จำนวนของสเกลลอปได้เพิ่มขึ้นตามการเพิ่มขึ้นของอัตราการไหล สเกลลอปนั้นถูกเชื่อว่าจะเกิดขึ้นจากข้อบกพร่องบนพื้นผิว และพบว่า ขนาดและจำนวนของสเกลลอปเพิ่มขึ้นตามการเพิ่มขึ้นของขนาดและความเข้มข้นของข้อบกพร่องบนพื้นผิวตามลำดับ อัตราการสลายตัวเฉลี่ยเพิ่มขึ้นตามการเพิ่มขึ้นของอัตราการไหล, ขนาดของอนุภาค, ความเข้มข้นของอนุภาค และอุณหภูมิ อัตราการสลายตัวของพลาสติกถูกควบคุมโดยจลศาสตร์แบบรวม (Mix Kinetics) และยังพบอีกว่าความเข้มข้นของพื้นผิวที่บกร่องนั้นมีผลต่อการสลายตัวของพลาสติกมากกว่าผลจากขนาดของพื้นผิวที่บกร่อง ความดันลดเพิ่มขึ้นตามการเพิ่มขึ้นของอัตราการไหลและอุณหภูมิ แต่ความดันลดลดลงตามการเพิ่มขึ้นของขนาดและความเข้มข้นของข้อบกพร่องบนพื้นผิว ซึ่งหมายความว่า เส้นผ่านศูนย์กลางของท่อพลาสติกมีผลมากกว่าผลจากความขรุขระบนพื้นผิว

ACKNOWLEDGEMENTS

First of all, I would like to thank my supervisor, Prof. Derek H. Lister, for giving me these great opportunities with his worth advice, knowledge and useful comments on my thesis work. I am grateful for his patience and kindness for giving me a chance to complete my research.

I would like to thank my supervisors, Prof. Frank R. Steward and Assoc. Prof. Thirasak Rirksomboon for their decision to take me as a graduate student and opportunity to do research in Canada and their support and advice.

This thesis work is funded by the Petroleum and Petrochemical College; and the National Center of Excellence for Petroleum, Petrochemicals, and Advanced Materials, Thailand.

Mr. Andrew Feicht and Mr. Piti Srisukvatananan are thanked for their technical advices, ideas and knowledge. I am grateful for providing all equipment throughout my work and solutions for any problems. Carl Murdock is thanks for all of his help providing the stuffs for my research work.

I would like to thank all graduate students in Chemical Engineering department and all my friends to help me in every ways to solve any problems. I have good memories and life in Canada because of you all.

Finally, this work could not been completed without my family. I would like to thank for their support and encouragement. Their love, supports and encouragement make me pass throughout the past year. I would also like to thank all my seniors and my friends in Thailand for their friendship and encouragement.

TABLE OF CONTENTS

	PAGE
Title Page	i
Abstract (in English)	iii
Abstract (in Thai)	iv
Acknowledgements	v
Table of Contents	vi
List of Tables	ix
List of Figures	xii
Abbreviations	xxvi
List of Symbols	xxvii
 CHAPTER	
I INTRODUCTION	1
 II LITERATURE REVIEW	 4
 III EXPERIMENTAL	 22
3.1 Materials and Equipment	22
3.1.1 Equipment	22
3.1.2 Chemicals	22
3.2 Methodology	22
3.2.1 Mixing	22
3.2.1.1 Mixing of the Plaster	22
3.2.1.2 Mixing sand grains with plaster of Paris	23
3.3 Test Section	24
3.4 Test Loop	24
3.5 Test Conditions	25
3.6 Analytical Techniques	27
3.6.1 Dissolution rate analysis	27

CHAPTER	PAGE
3.6.1.1 Dissolution rate with time from mass variations	27
3.6.1.2 Dissolution rate with time by using atomic absorption spectrophotometer (AAS)	27
3.6.1.3 Dissolution rate along the pipe	28
3.6.2 Pressure drop analysis	28
3.6.3 Characterization of scalloped surface	28
3.6.4 Determination of the gypsum dissolution	28
 IV RESULTS AND DISCUSSION	 30
4.1 Scallop Surface	30
4.1.1 The Effect of pH	30
4.1.2 The Effect of Flow Rate	33
4.1.3 The Effect of Initial Presence of Defects	33
4.1.3.1 Effect of Particle Size	34
4.1.3.2 Effect of Particle Concentration	34
4.1.4 The Effect of Temperature	35
4.2 Dissolution Rate	36
4.2.1 Dissolution Rate with Time	36
4.2.1.1 The Effect of pH	36
4.2.1.2 The Effect of Flow Rate	42
4.2.1.3 The Effect of Particle Size	42
4.2.1.4 The Effect of Particle Concentration	45
4.2.1.5 The Effect of Temperature	47
4.2.2 Dissolution Rate Along the Pipe Length	49
4.2.2.1 The Effect of pH	49
4.2.2.2 The Effect of Flow Rate	52
4.2.2.3 The Effect of Particle Size	52
4.2.2.4 The Effect of Particle Concentration	54
4.2.1.5 The Effect of Temperature	56

CHAPTER	PAGE
4.3 Pressure Drop	57
4.3.1 The Effect of pH	57
4.3.2 The Effect of Flow Rate	58
4.3.3 The Effect of Particle Size	59
4.3.4 The Effect of Particle Concentration	60
4.3.5 The Effect of Temperature	61
4.4 The Mechanism of Gypsum Dissolution	62
4.4.1 The Effect of pH	63
4.4.2 The Effect of Flow Rate	64
4.4.3 The Effect of Particle Size	66
4.4.4 The Effect of Particle Concentration	67
4.4.5 The Effect of Temperature	69
4.5 Effects of various Parameters on Dissolution	71
V CONCLUSIONS AND RECOMMENDATIONS	74
REFERENCES	76
APPENDICES	79
Appendix A Dissolution Rate	79
Appendix B Pressure Drop	106
Appendix C The Mechanism of Gypsum Dissolution	116
CURRICULUM VITAE	129

LIST OF TABLES

TABLE		PAGE
3.1	Conditions for studying the effects of pH and flow rate (pure plaster – no defects).	26
3.2	Conditions for studying the effects of temperature, particle size, defect concentration and flow rate.	26
4.1	Average dissolution rate calculated from AAS at different pHs and 25LPM.	39
4.2	Average dissolution rate calculated from AAS at different pHs and 35 LPM.	41
4.3	Average dissolution rate calculated from AAS at different sizes of initial defects and 25 LPM and 25°C.	44
4.4	Average dissolution rate calculated from AAS at different sizes of initial defects and 35 LPM and 25°C.	44
4.5	Average dissolution rate calculated from AAS at different concentrations of initial defects at defect size of 0.500-0.707 mm, 25LPM and 25°C.)	46
4.6	Average dissolution rate calculated from AAS at different concentrations of initial defects at defect size of 0.500-0.707 mm and 35LPM and 25°C.	47
4.7	Average dissolution rate calculated from the thickness of pipe at different pHs and different flowrates.	52
4.8	Average dissolution rate calculating from the thickness of pipe at different sizes of initial defects and different flowrates.	54
4.9	Average dissolution rate calculating from the thickness of pipe at different concentrations of initial defects and different flowrates.	56

TABLE	PAGE
4.10 Values of dissolution rate constant, mass transfer coefficient and dissolution coefficient at different pHs.	65
4.11 Average values of mass transfer coefficient and dissolution coefficient at different surface roughness.	68
4.12 Average values of mass transfer coefficient and dissolution coefficient at different temperatures.	70
4.13 Average values of mass transfer coefficient and dissolution coefficient at different temperatures.	70
4.14 Dissolution rate comparison between the effect of flow rate and effect of temperature.	72
4.15 Dissolution rate comparison between the effect of initial defect size and effect of initial defect concentration.	73
A.1 Average dissolution rate calculating from AAS at different sizes of initial defects and 25 LPM.	81
A.2 Average dissolution rate calculating from AAS at different sizes of initial defects and 35 LPM.	82
A.3 Average dissolution rate calculating from AAS at different concentrations of initial defects at defect size of 0.21-0.25 mm and 25LPM.	84
A.4 Average dissolution rate calculating from AAS at different concentrations of initial defects at defect size of 0.42-0.50 mm and 25LPM.	85
A.5 Average dissolution rate calculating from AAS at different concentrations of initial defects at defect size of 0.21-0.25 mm and 35LPM.	86
A.6 Average dissolution rate calculating from AAS at different concentrations of initial defects at defect size of 0.42-0.50 mm and 35LPM.	87

TABLE		PAGE
A.7	Average dissolution rate calculating from AAS at different sizes of initial defects and 35 LPM.	96
A.8	Average dissolution rate calculating from the thickness of pipe at different concentrations of initial defects and different flowrate.	97
A.9	Average dissolution rate calculating from the thickness of pipe at different concentrations of initial defects and different flowrate.	99

LIST OF FIGURES

FIGURE		PAGE
1.1	Scallops found on outlet feeder pipe k16 (Lister, 2004).	2
2.1	Scalloping on the inner surface of a carbon steel feeder pipe (Villien <i>et al.</i> , 2001)	5
2.2	Schematic of primary coolant in a CANDU reactor	6
2.3	Evolution of a surface, (1) passive-bed theory and (2) defect theory	8
2.4	Stages in the development of experimental flutes (a-e) and grooves (f), (g) defects introduced into Plaster of Paris beds. Flow from bottom to top. (e) 10cmwidth (Allen, 1971).	10
2.5	Flute hydrodynamics (Blumberg, 1970)	11
2.6	SEM of the plaster structure.	12
2.7	Dissolution rates of gypsum as functions of flow rate (Villien <i>et al.</i> , 2005).	15
2.8	Concentration of calcium ion vs time for four experiments, each run at 300-rpm spinning rate and 25°C (Raines and Dewers, 1997)	16
2.9	Schematic of different scallop types at inlet and outlet (Shao, 2006).	16
2.10	Dihydrate solubility in H ₂ O vs. temperature. The curve is determined from the OLI default database (Azimi <i>et al.</i> , 2007)	17
2.11	The 1000/T dependence of log k (dissolution rate constant) of different specimens or different kinds of gypsum (Lebedev, <i>et al.</i> 1989).	18
2.12	The pressure drop versus time (Shao, 2006)	18

FIGURE		PAGE
2.13	Gypsum solubility in H ₂ SO ₄ solutions at different temperatures.	20
2.14	Dependence of Ca ²⁺ concentration on the OH ⁻ concentration in the solution with and without sulphate.	20
2.15	Comparison of dissolution rates at different pHs.	21
3.1	Schematic of the mixing apparatus.	23
3.2	Schematic of the test section. (Villien, <i>et al.</i> , 2005)	24
3.3	Schematic of the experimental loop.	25
4.1	Scallop formation on defect-free plaster surface every hour at different pHs, 25 LPM and 30°C: (a1) – (a5) run at pH3, (b1) – (b5) run at pH7, (c1) – (c5) run at pH10.	31
4.2	Scallop formation on defect-free plaster surface every hour at different pHs, 35 LPM and 30°C: (a1) – (a5) run at pH3, (b1) – (b5) run at pH7, (c1) – (c5) run at pH10.	32
4.3	Scallop formation on defect-free plaster surface at different flow rates at pH 7, 30°C: (a) 25 LPM (b) 35LPM.	33
4.4	Scallop formation on plaster surface at different sizes of initial defects at 25°C, 25LPM and 50 defects/cm ³ : (a) pure plaster (b) 0.21-0.25mm (c) 0.42-0.50mm and (d) 0.505-0.707mm.	34
4.5	Scallop formation on plaster surface at different concentrations of initial defects at 25°C, 25LPM. 0.500-0.707 mm: (a) 50 defects/cm ³ (b) 100 defects/cm ³ .	35
4.6	Scallop formation on plaster surface at different temperatures at 25LPM, 0.42-0.50 mm and 50 defects/cm ³ : (a) 25°C (b) 10 °C.	36

FIGURE	PAGE
4.7 The effects of pH on the dissolution rate of plaster with time, 25LPM, 30°C.	38
4.8 The effect of pH on the dissolution rate of plaster of Paris with time at 35LPM, 30°C.	40
4.9 Effect of flow rate on the dissolution rate with time at pH3 and 30°C.	42
4.10 Dissolution rate with time at different sizes of particles, 25°C, 50 defects/cm ³ and 25LPM.	43
4.11 Dissolution rate with time at different sizes of particles, 25°C, 50 defects/cm ³ and 35LPM.	43
4.12 Dissolution rate with time at different concentrations of particles, 0.500-0.707 mm, 25°C and 25LPM.	45
4.13 Dissolution rate with time at different concentrations of particles, 0.500-0.707 mm 25°C and 35LPM.	45
4.14 Dissolution rate with time at different temperatures, 0.21-0.25 mm, 50 defects/cm ³ and 25LPM.	48
4.15 Dissolution rate with time at different temperatures, 0.21-0.25 mm, 50 defects/cm ³ and 35LPM.	48
4.16 Dissolution along the pipe at 25LPM, 30°C.	49
4.17 Dissolution along the pipe at 35LPM, 30°C.	50
4.18 Plaster test section at different positions (a) 25 LPM at the entrance, (b) 25 LPM at the exit, (c) 35 LPM at the entrance, (d) 35 LPM at the exit.	51
4.19 Dissolution rate along the pipe length at pH3 and 30°C.	52
4.20 Dissolution along the pipe at different particle sizes, 50 defects/cm ³ , 25LPM and 25°C.	53
4.21 Dissolution along the pipe at different particle sizes, 50 defects/cm ³ , 35LPM and 25°C.	53

FIGURE	PAGE	
4.22	Dissolution along the pipe at different particle concentrations, 0.500-0.707 mm, 25LPM and 25°C.	55
4.23	Dissolution along the pipe at different particle concentrations, 0.500-0.707 mm, 35LPM and 25°C.	55
4.24	Dissolution along the pipe at different temperatures, 0.21-0.25 mm, 50 defects/cm ³ , 25LPM.	56
4.25	Pressure drop with time at 25 LPM, 30°C.	57
4.26	Pressure drop with time at 35 LPM, 30°C.	58
4.27	Pressure drop with time at pH3, 30°C.	58
4.28	Pressure drop at different sizes of particles, 50 defects/cm ³ , 25°C and 25 LPM.	59
4.29	Pressure drop at different sizes of particles, 50 defects/cm ³ , 25°C and 35 LPM.	60
4.30	Pressure drop with time at different concentrations of particles, 0.42-0.50 mm, 25°C and 25 LPM.	60
4.31	Pressure drop with time at different concentrations of particles, 0.42-0.50 mm, 25°C and 35 LPM.	61
4.32	Pressure drop with time at different temperatures, 0.21-0.25 mm, 50 defects/cm ³ and 25 LPM.	61
4.33	Pressure drop with time at different temperatures, 0.21-0.25 mm, 50 defects/cm ³ and 35 LPM.	62
4.34	The overall rate constant (K) and the dissolution coefficient (k _d) compared with the mass transfer coefficient (k _m) along the pipe under condition pH3, 30°C and 25 LPM	63
4.35	The overall rate constant (K) and the dissolution coefficient (k _d) compared with the mass transfer coefficient (k _m) along the pipe under condition pH7, 30°C and 25 LPM	63

FIGURE		PAGE
4.36	The overall rate constant (K) and the dissolution coefficient (k_d) compared with the mass transfer coefficient (k_m) along the pipe under condition pH10, 30°C and 25 LPM	64
4.37	The overall rate constant (K) and the dissolution coefficient (k_d) compared with the mass transfer coefficient (k_m) along the pipe under condition pH3, 30°C and 25 LPM	64
4.38	The overall rate constant (K) and the dissolution coefficient (k_d) compared with the mass transfer coefficient (k_m) along the pipe under condition pH3, 30°C and 35 LPM	65
4.39	The overall rate constant (K) and the dissolution coefficient (k_d) compared with the mass transfer coefficient (k_m) along the pipe under condition 0.21-0.25mm, 50 defects/cm ³ , 25°C and 25 LPM.	66
4.40	The overall rate constant (K) and the dissolution coefficient (k_d) compared with the mass transfer coefficient (k_m) along the pipe under condition 0.42-0.50mm, 50 defects/cm ³ , 25°C and 25 LPM.	66
4.41	The overall rate constant (K) and the dissolution coefficient (k_d) compared with the mass transfer coefficient (k_m) along the pipe under condition 0.500-0.707 mm, 50 defects/cm ³ , 25°C and 25 LPM.	67
4.42	The overall rate constant (K) and the dissolution coefficient (k_d) compared with the mass transfer coefficient (k_m) along the pipe under condition 0.42-0.50mm, 50 defects/cm ³ , 25°C and 25 LPM.	67

FIGURE	PAGE
4.43 The overall rate constant (K) and the dissolution coefficient (k_d) compared with the mass transfer coefficient (k_m) along the pipe under condition 0.42-0.50mm, 100 defects/cm ³ , 25°C and 25 LPM.	68
4.44 The overall rate constant (K) and the dissolution coefficient (k_d) compared with the mass transfer coefficient (k_m) along the pipe under condition 0.42-0.50mm, 50 defects/cm ³ , 10°C and 25 LPM.	69
4.45 The overall rate constant (K) and the dissolution coefficient (k_d) compared with the mass transfer coefficient (k_m) along the pipe under condition 0.42-0.50mm, 50 defects/cm ³ , 25°C and 25 LPM.	69
A.1 Dissolution rate with time at pH7 and 30°C.	79
A.2 Dissolution rate with time at pH10 and 30°C.	80
A.3 Dissolution rate with time at different sizes of particles, 25°C, 100 defects/cm ³ and 25LPM.	80
A.4 Dissolution rate with time at different sizes of particles, 25°C, 100 defects/cm ³ and 35LPM.	81
A.5 Dissolution rate with time at different concentrations of particles, 0.21-0.25 mm, 25°C and 25LPM.	83
A.6 Dissolution rate with time at different concentrations of particles, 0.42-0.50 mm, 25°C and 25LPM.	83
A.7 Dissolution rate with time at different concentrations of particles, 0.21-0.25 mm, 25°C and 35LPM.	85
A.8 Dissolution rate with time at different concentrations of particles, 0.42-0.50 mm, 25°C and 35LPM.	86
A.9 Dissolution rate with time at different temperatures, pure plaster and 25LPM.	88

FIGURE	PAGE
A.10	Dissolution rate with time at different temperatures, pure plaster and 35LPM. 88
A.11	Dissolution rate with time at different temperatures, 0.42-0.50 mm, 50 defects/cm ³ and 25LPM. 89
A.12	Dissolution rate with time at different temperatures, 0.42-0.50 mm, 50 defects/cm ³ and 35LPM. 89
A.13	Dissolution rate with time at different temperatures, 0.500-0.707 mm, 50defects/cm ³ and 25LPM. 90
A.14	Dissolution rate with time at different temperatures, 0.500-0.707 mm, 50 defects/cm ³ and 35LPM. 90
A.15	Dissolution rate with time at different temperatures, 0.21-0.25 mm, 100 defects/cm ³ and 25LPM. 91
A.16	Dissolution rate with time at different temperatures, 0.21-0.25 mm, 100 defects/cm ³ and 35LPM. 91
A.17	Dissolution rate with time at different temperatures, 0.42-0.50 mm, 100 defects/cm ³ and 25LPM. 92
A.18	Dissolution rate with time at different temperatures, 0.42-0.50 mm, 100 defects/cm ³ and 35LPM. 92
A.19	Dissolution rate with time at different temperatures, 0.500-0.707 mm, 100 defects/cm ³ and 25LPM. 93
A.20	Dissolution rate with time at different temperatures, 0.500-0.707 mm, 100 defects/cm ³ and 35LPM. 93
A.21	Dissolution rate along the pipe length under pH7 and 30°C. 94
A.22	Dissolution rate along the pipe length under pH10 and 30°C. 94
A.23	Dissolution along the pipe at different particle sizes, 100 defects/cm ³ , 25LPM and 25°C. 95

FIGURE		PAGE
A.24	Dissolution along the pipe at different particle sizes, 100 defects/cm ³ , 35LPM and 25°C.	95
A.25	Dissolution along the pipe at different particle concentrations, 0.21-0.25 mm, 25LPM and 25°C.	96
A.26	Dissolution along the pipe at different particle concentrations, 0.21-0.25 mm, 35LPM and 25°C.	97
A.27	Dissolution along the pipe at different particle concentrations, 0.42-0.50 mm, 25LPM and 25°C.	98
A.28	Dissolution along the pipe at different particle concentrations, 0.42-0.50 mm, 35LPM and 25°C.	98
A.29	Dissolution along the pipe at different temperatures, pure plaster, and 25LPM.	99
A.30	Dissolution along the pipe at different temperatures, pure plaster, and 35LPM.	100
A.31	Dissolution along the pipe at different temperatures, 0.21-0.25, 50 defects/cm ³ and 35LPM.	100
A.32	Dissolution along the pipe at different temperatures, 0.42-0.50, 50 defects/cm ³ and 25LPM.	101
A.33	Dissolution along the pipe at different temperatures, 0.42-0.50, 50 defects/cm ³ and 35LPM.	101
A.34	Dissolution along the pipe at different temperatures, 0.500-0.707, 50 defects/cm ³ and 25LPM.	102
A.35	Dissolution along the pipe at different temperatures, 0.500-0.707, 50 defects/cm ³ and 35LPM.	102
A.36	Dissolution along the pipe at different temperatures, 0.21-0.25, 100 defects/cm ³ and 25LPM.	103

FIGURE	PAGE
A.37 Dissolution along the pipe at different temperatures, 0.21-0.25, 100 defects/cm ³ and 35LPM.	103
A.38 Dissolution along the pipe at different temperatures, 0.42-0.50, 100 defects/cm ³ and 25LPM.	104
A.39 Dissolution along the pipe at different temperatures, 0.42-0.50, 100 defects/cm ³ and 35LPM.	104
A.40 Dissolution along the pipe at different temperatures, 0.500-0.707, 100 defects/cm ³ and 25LPM.	105
A.41 Dissolution along the pipe at different temperatures, 0.500-0.707, 100 defects/cm ³ and 35LPM.	105
B.1 Pressure drop under pH7 and 30°C.	106
B.2 Pressure drop under pH10 and 30°C.	106
B.3 Pressure drop at different sizes of particles, 100 defects/cm ³ , 25°C and 25 LPM.	107
B.4 Pressure drop at different sizes of particles, 100 defects/cm ³ , 25°C and 35 LPM.	107
B.5 Pressure drop with time at different concentrations of particles, 0.21-0.25 mm, 25°C and 25 LPM.	108
B.6 Pressure drop with time at different concentrations of particles, 0.21-0.25 mm, 25°C and 35 LPM.	108
B.7 Pressure drop with time at different concentrations of particles, 0.500-0.707 mm, 25°C and 25 LPM.	109
B.8 Pressure drop with time at different concentrations of particles, 0.500-0.707 mm, 25°C and 35 LPM.	109
B.9 Pressure drop with time at different temperatures, pure plaster and 25 LPM.	110
B.10 Pressure drop with time at different temperatures, pure plaster and 35 LPM.	110

FIGURE	PAGE
B.11 Pressure drop with time at different temperatures, 0.42-0.50, 50 defects/cm ³ and 25 LPM.	111
B.12 Pressure drop with time at different temperatures, 0.42-0.50, 50 defects/cm ³ and 35 LPM.	111
B.13 Pressure drop with time at different temperatures, 0.500-0.707, 50 defects/cm ³ and 25 LPM.	112
B.14 Pressure drop with time at different temperatures, 0.500-0.707, 50 defects/cm ³ and 35 LPM.	112
B.15 Pressure drop with time at different temperatures, 0.21-0.25, 100 defects/cm ³ and 25 LPM.	113
B.16 Pressure drop with time at different temperatures, 0.21-0.25, 100 defects/cm ³ and 35 LPM.	113
B.17 Pressure drop with time at different temperatures, 0.42-0.50, 100 defects/cm ³ and 25 LPM.	114
B.18 Pressure drop with time at different temperatures, 0.42-0.50, 100 defects/cm ³ and 35 LPM.	114
B.19 Pressure drop with time at different temperatures, 0.500-0.707, 100 defects/cm ³ and 25 LPM.	115
B.20 Pressure drop with time at different temperatures, 0.500-0.707, 100 defects/cm ³ and 35 LPM.	115
C.1 The overall rate constant (K) and the dissolution coefficient (k _d) compared with the mass transfer coefficient (k _m) along the pipe length under condition pH7, 30°C and 25 LPM.	116
C.2 The overall rate constant (K) and the dissolution coefficient (k _d) compared with the mass transfer coefficient (k _m) along the pipe length under condition pH7, 30°C and 35 LPM.	117

FIGURE	PAGE
C.3 The overall rate constant (K) and the dissolution coefficient (k_d) compared with the mass transfer coefficient (k_m) along the pipe length under condition pH10, 30°C and 25 LPM.	117
C.4 The overall rate constant (K) and the dissolution coefficient (k_d) compared with the mass transfer coefficient (k_m) along the pipe length under condition pH10, 30°C and 35 LPM.	118
C.5 The overall rate constant (K) and the dissolution coefficient (k_d) compared with the mass transfer coefficient (k_m) the pipe length under condition 0.21-0.25 mm, 100 defects/cm ³ , 25°C and 25 LPM.	118
C.6 The overall rate constant (K) and the dissolution coefficient (k_d) compared with the mass transfer coefficient (k_m) along the pipe length under condition 0.42-0.50 mm, 100 defects/cm ³ , 25°C and 25 LPM.	119
C.7 The overall rate constant (K) and the dissolution coefficient (k_d) compared with the mass transfer coefficient (k_m) along the pipe length under condition 0.500-0.707 mm, 100 defects/cm ³ , 25°C and 25 LPM.	119
C.8 The overall rate constant (K) and the dissolution coefficient (k_d) compared with the mass transfer coefficient (k_m) along the pipe length under condition 0.21-0.25 mm, 50 defects/cm ³ , 25°C and 25 LPM.	120
C.9 The overall rate constant (K) and the dissolution coefficient (k_d) compared with the mass transfer coefficient (k_m) along the pipe length under condition 0.21-0.25 mm, 100 defects/cm ³ , 25°C and 25 LPM.	120

FIGURE	PAGE
C.10 The overall rate constant (K) and the dissolution coefficient (k_d) compared with the mass transfer coefficient (k_m) along the pipe length under condition 0.500-0.707 mm, 50 defects/cm ³ , 25°C and 25 LPM.	121
C.11 The overall rate constant (K) and the dissolution coefficient (k_d) compared with the mass transfer coefficient (k_m) along the pipe length under condition 0.500-0.707 mm, 100 defects/cm ³ , 25°C and 25 LPM.	121
C.12 The overall rate constant (K) and the dissolution coefficient (k_d) compared with the mass transfer coefficient (k_m) along the pipe length under condition pure plaster, 10°C and 25 LPM.	122
C.13 The overall rate constant (K) and the dissolution coefficient (k_d) compared with the mass transfer coefficient (k_m) along the pipe length under condition 0.21-0.25 mm, 100 defects/cm ³ , 10°C and 25 LPM.	122
C.14 The overall rate constant (K) and the dissolution coefficient (k_d) compared with the mass transfer coefficient (k_m) along the pipe length under condition 0.42-0.50 mm, 50 defects/cm ³ , 10°C and 25 LPM.	123
C.15 The overall rate constant (K) and the dissolution coefficient (k_d) compared with the mass transfer coefficient (k_m) along the pipe length under condition 0.42-0.50 mm, 100 defects/cm ³ , 10°C and 25 LPM.	123
C.16 The overall rate constant (K) and the dissolution coefficient (k_d) compared with the mass transfer coefficient (k_m) along the pipe length under condition 0.500-0.707 mm, 50 defects/cm ³ , 10°C and 25 LPM.	124

FIGURE		PAGE
C.17	The overall rate constant (K) and the dissolution coefficient (k_d) compared with the mass transfer coefficient (k_m) along the pipe length under condition 0.500-0.707 mm, 100 defects/cm ³ , 10°C and 25 LPM.	124
C.18	The overall rate constant (K) and the dissolution coefficient (k_d) compared with the mass transfer coefficient (k_m) along the pipe length under condition pure plaster, 10°C and 35 LPM.	125
C.19	The overall rate constant (K) and the dissolution coefficient (k_d) compared with the mass transfer coefficient (k_m) along the pipe length under condition 0.21-0.25 mm, 50 defects/cm ³ , 10°C and 35 LPM.	125
C.20	The overall rate constant (K) and the dissolution coefficient (k_d) compared with the mass transfer coefficient (k_m) along the pipe length under condition 0.21-0.25 mm, 100 defects/cm ³ , 10°C and 35 LPM.	126
C.21	The overall rate constant (K) and the dissolution coefficient (k_d) compared with the mass transfer coefficient (k_m) along the pipe length under condition 0.42-0.50 mm, 50 defects/cm ³ , 10°C and 35 LPM.	126
C.22	The overall rate constant (K) and the dissolution coefficient (k_d) compared with the mass transfer coefficient (k_m) along the pipe length under condition 0.42-0.50 mm, 100 defects/cm ³ , 10°C and 35LPM.	127
C.23	The overall rate constant (K) and the dissolution coefficient (k_d) compared with the mass transfer coefficient (k_m) along the pipe length under condition 0.500-0.707 mm, 50 defects/cm ³ , 10°C and 35LPM.	127

FIGURE	PAGE
C.24 Mass The overall rate constant (K) and the dissolution coefficient (k_d) compared with the mass transfer coefficient (k_m) along the pipe length under condition 0.500-0.707 mm, 100 defects/cm ³ , 10°C and 35LPM.	128